

## Characterization of KCl-Activated Carbon Derived from Walnut Shells of Tidore Island, Indonesia

*I Dewe Ketut Anom*<sup>\*1</sup>  , *Chaleb Paul Maanari*<sup>1</sup>  , *Marianus*<sup>2</sup>  , *Johny Zeth Lombok*<sup>1</sup>  , *Saprizal Hadisaputra*<sup>3</sup>  , *I Dewa Gede Katja*<sup>4</sup>  , *Jefry Jack Mamangkey*<sup>5</sup>  , *Aisyiah Restutiningsih Putri Utami*<sup>1</sup>  

<sup>1</sup>Department of Chemistry, Faculty of Mathematics and Natural Sciences, Universitas Negeri Manado, Indonesia.

<sup>2</sup>Department of Physics, Faculty of Mathematics and Natural Sciences, Universitas Negeri Manado, Indonesia.

<sup>3</sup>Chemistry Education Division, Faculty of Teacher Training and Education, University of Mataram, Indonesia.

<sup>4</sup>Department of Chemistry, Faculty of Mathematics and Natural Sciences, Sam Ratulangi University, Indonesia.

<sup>5</sup>Department of Biology, Faculty of Mathematics and Natural Sciences, Universitas Negeri Manado, Indonesia.

\*Corresponding Author.

Received 15/01/2024, Revised 27/09/2024, Accepted 29/09/2024, Published Online First 20/12/2024



© 2022 The Author(s). Published by College of Science for Women, University of Baghdad.

This is an open-access article distributed under the terms of the [Creative Commons Attribution 4.0 International License](https://creativecommons.org/licenses/by/4.0/), which permits unrestricted use, distribution, and reproduction in any medium, provided the original work is properly cited.

### Abstract

Activated carbon is highly valued for its versatility and extensive industrial use. Walnut (*Canarium vulgare* Leech), an indigenous Indonesian plant primarily found in Eastern regions like Maluku and Tidore islands, produces shells that can be converted into activated carbon. This study involved obtaining carbon from walnut shells through pyrolysis at 360°C for 6 hours, followed by activation in a 3M KCl solution for 24 hours. The activated carbon was analyzed using Fourier Transform Infrared Spectroscopy (FTIR), Scanning Electron Microscopy-Energy Dispersive X-ray (SEM-EDX), and X-ray Diffraction (XRD). FTIR analysis revealed functional groups including N-H, Ar-H (aromatic), C≡N, carbonyl CO, and ester CO. SEM images showed a non-homogeneous structure in pyrolyzed and KCl-activated carbon. After activation, the pore diameter distribution increased significantly from 496.2 nm to 1,226 μm. EDX analysis indicated a rise in carbon content from 85.40% after pyrolysis to 86.50% post-KCl activation. XRD diffractograms suggested amorphous structures in both forms of carbon, as indicated by loose peaks and broad diffraction patterns. This research introduces the novel use of KCl as an activator to enhance the porosity of walnut shell-derived activated carbon. The KCl-activated carbon demonstrated an ability to remove 0.122 mg/L of Fe(III), achieving 16.78% Fe(III) absorption in 150 minutes. These findings suggest that KCl-activated walnut shell carbon could be an effective alternative absorbent for clean water treatment in the future.

**Keywords:** Carbon, FTIR, KCl-Activator, SEM-EDX, Walnut shells, XRD

### Introduction

A walnut shell is a part of a walnut that is not utilized by people and is disposed of as waste. Hence, it is considered to have no economic value. The abundance of walnut shells is a natural biomass material considered waste and has no economic value. If these walnut shells are not processed or utilized into useful products, the waste can affect environmental sustainability<sup>1</sup>. Walnut shell has a

solid physical structure that is good enough to be used as carbon. Around 86 tons of walnut shells annually in Indonesia are not utilized optimally; some are only used as firewood. Turkey is the fourth largest producer of walnuts, producing 180,807 tons of walnuts in 2014. The potential number of walnut shells in Turkey can be estimated at 96,732 tons annually. It is not used in industry except to be

burned directly, and the rest is discarded away<sup>2</sup>. The surface and shells of walnut seeds are the primary source of lignocellulosic. This agricultural waste has become the primary source of porous carbon for environmental protection and ecological sustainability<sup>3-5</sup>. Waste materials such as walnut shells, coconut shells, chitosan, and rice husks are used for porous carbon because the carbohydrate structure is renewable<sup>6,7</sup>. Walnut shells have been reported to be produced into activated carbon by pyrolysis<sup>8</sup>. The chemical composition of the walnut shell consists of 39.24% cellulose, 38.00% lignin, 11.72% water, 9.25% hemicellulose, and 1.79% ash, extractives (10.2%); the highest amount belongs to water extractives 4.6%, followed by dichloromethane 2.9% and ethanol 2.7%<sup>9</sup>. The main products from the pyrolysis of walnut shells are 36.80% charcoal, 42.58% liquid smoke, 4.48% tar, and 15.79% incondensable volatile gas components<sup>10</sup>. Walnut shells carbon has hydroxyl groups (R-OH), carbonyl groups (RC=O), esters (R-CO-OR'), alkanes (R-CH<sub>2</sub>), carboxyl groups (R-COOH) and aromatic groups (R-CH)<sup>11,12</sup>. Besides generating carbon, this heating or decomposition process produces gases, liquids, smoke, and carbon<sup>13</sup>.

Walnut is a Juglandaceae regia tree family and belongs to the dried fruit family. Farmers widely cultivate walnuts because they are a nutrient source for people, but it has resulted in a lot of waste in the form of walnut shells, which have been thrown away. Research about converting walnut shells into useful substances has been widely developed. Based on the research, the walnut shell can be used as a supercapacitor device. The method converts walnut shells into an energy storage approach, the morphologies of walnut shells provide a large surface area in the form of mesopores or micropores, and the last is the easy preparation method<sup>14</sup>. The other advantage of walnut shells is as an adsorbent. First, the walnut shell is processed to become activated carbon and is applied as an iodine gas capture. Walnut shells have a lot of advantages, mainly because they are low cost, have easy preparation processes, and have a large surface area<sup>15</sup>. Walnut shells' activated carbon is widely used as an adsorbent. Another research study showed that walnut shell-activated carbon can be used as a hydrogen gas adsorbent. The characteristics of walnut shells make them suitable for adsorption and have many other advantages. Low-cost walnut shell-based carbons are activated by potassium hydroxide

and produce activated walnut shell carbon with a large surface area in the form of microporosity. It is one of the promising advantages and processes of walnut shell waste. The process follows a carbon capture system and storage to reduce CO<sub>2</sub> emissions from industry or motor vehicle waste to the atmosphere. Based on this case, so the selective adsorbent must be chosen. The characteristics of the adsorbent should be solid material, low cost, excellent and high surface area, large pore volume, good thermal and chemical stability, ability to be recycled, excellent mechanical resistance, affinity towards CO<sub>2</sub>, and faster kinetics. Walnut shells' activated carbon can also be used in food, beverage, and automobile<sup>16</sup>. The other research on activated carbon walnut shell-based is as a monoethanolamine (MEA) bio-adsorbent solution to enhance carbon dioxide absorption. This research successfully used the walnut shell from walnut trees in the Anzali Port of Iran<sup>17</sup>.

Pyrolysis is a heating process at a high temperature or a predetermined temperature in a room without oxygen, and activation is how to activate the carbon using chemicals<sup>18</sup>. The activation process aims at the pore-diameter carbons<sup>19</sup>. Activation is required for the porosity of the carbon and increasing the surface area of the activated carbon<sup>20</sup>. Activated carbon can be obtained through chemical processes, such as KOH, NaOH, K<sub>2</sub>CrO<sub>3</sub>, ZnCl<sub>2</sub>, FCl<sub>3</sub>, H<sub>2</sub>SO<sub>4</sub>, HCl and H<sub>3</sub>PO<sub>4</sub><sup>21-24</sup>. Among the existing hydroxy alkalis (NaOH, LiOH, and KOH), KOH is the most effective activator widely studied<sup>25-28</sup>. Active hydrochar H<sub>3</sub>PO<sub>4</sub> derived from hickory wood and peanut shells has been previously reported, and it was found that the chemical modification significantly increased the adsorption capacity of the hydrochar to acetone and cyclohexane<sup>20,29</sup>. The nature of activated carbon is widely used as an adsorbent or adsorbent in the pharmaceutical and food industries<sup>30,31</sup>.

In this study, walnut shells were taken from the mountains in the Tidore Islands Regency. This study aims to synthesize the activated carbon from walnut skin waste through pyrolysis and activate it with potassium chloride solution (KCl). KCl has been used as a chemical activator in manufacturing activated carbon from cassava peels<sup>32</sup>. Due to its relatively high absorption capacity for iodine of 792.427 mg/g and absorption capacity for methylene blue of 19.925 mg/g<sup>33</sup>. After the carbonization process, the carbon is activated chemically with the help of a chemical solution such as an H<sub>2</sub>SO<sub>4</sub>, KOH and KCl solution<sup>33-36</sup>. The KCl activator is a

substance or chemical compound that functions as an activating reagent, and this substance activates the carbon atoms to improve their absorption capacity. Based on a literature search, KCl is not used as an activator to make activated charcoal, especially from walnut shells. The resulting synthesis of activated walnut shell charcoal will be applied as an absorbent to absorb iron in drilled well water from Tataaran Tondano village.

Compared to other activators, the advantage of using the KCl activator is that KCl binds water and causes the water firmly bound to the carbon pores to be released during carbonization. The KCl activator will enter the pores and open the closed charcoal surface. Apart from the KCl activator, it can open closed pores and create new ones. Thus, when heating is

carried out, the impurity compounds in the pores become more easily absorbed so that the surface area of the activated carbon becomes larger and increases its absorption capacity. Walnut shell carbon resulting from pyrolysis and chemical activation was analyzed using Fourier Transform Infrared (FT-IR), Scanning Electron Microscope (SEM)<sup>37</sup>, Energy Dispersive X-ray (EDX), X-ray diffraction (XRD) and ASC-7000 Shimadzu instruments<sup>38</sup>. Meanwhile, this research used the pyrolysis method and fragmentation of KCl-activated walnut shell carbon powder to produce activated carbon with a macro-pore size of 1,020-1,226  $\mu\text{m}$ . This research's novelty is that no information explicitly using KCl activator to increase the porosity of activated carbon from walnut shells is available.

## Materials and Methods

### Tools and materials

The research was conducted from April to September 2023. The preparation and pyrolysis occurred at the Chemistry Laboratory of Universitas Negeri Manado, North Sulawesi, Indonesia. The characterization analysis was conducted at the Chemistry Laboratory of Universitas Negeri Malang, Surabaya, Indonesia.

The tools used were glassware, porcelain cups, 100 mesh sieve, desiccators, crucibles, mortar, pestle, oven (Mettler UN110), and furnace (Thermo Scientific Lindberg/Blue). Fourier Transform Infrared Spectrophotometer (FTIR) Shimadzu IRPrestige-21 (Japan), Scanning Electron Microscope-Energy Dispersive X-Ray (SEM-EDX) FEI Inspect-S50 (USA), and X-Ray Diffraction (XRD) PANalytical X'Pert PRO (Netherlands) were recorded at the Chemistry Laboratory of Universitas Negeri Malang and ASC-7000, AAS Shimadzu (Japan) at the Class I Environmental Health and Disease Control Center.

The materials used were walnut shells from the Tidore Islands district, North Maluku, Indonesia, potassium chloride (ACS reagent,  $\geq 99\%$ , powder) was purchased from Sigma-Aldrich, distilled water (WaterOne,  $\geq 99\%$  purity), and other chemicals.

### Methods

#### Sample preparation

Walnut shell samples (3 kg) were separated from their outside fruit skin, cleaned, and dried under the sunlight to remove water content. Walnut shells were pyrolyzed at the temperature of 350  $^{\circ}\text{C}$  for 6 hours.

The walnut shell carbon (WSC) was allowed to cool before being ground using a mortar. After that, the grounded WSC (500 g) was sieved (100 mesh). As much as 20 g of sieved WSC was soaked in 3M KCl solution for 24 hours, and then it was washed with distilled water until pH became neutral at  $\pm 7$ . The residue dried in an oven at 110-120  $^{\circ}\text{C}$  for 4 hours. Subsequently, it was stored in a desiccator until the carbon stabilizes<sup>29</sup>.

#### FTIR analysis

The sample preparation for FTIR measurements involved creating KBr pellets using a ratio of 1:10 (carbon: KBr). The FT-IR measurements were conducted using the FTIR Shimadzu type IRprestige-21 (Japan) at the Materials Laboratory, University of Malang. The spectrophotometer works within a scan range of 4000-400  $\text{cm}^{-1}$ , a resolution of 4  $\text{cm}^{-1}$ , and a scan of 4.0 s. The IR Solution application was utilized for spectrum measurements, peak detection, and determination of functional groups.

#### SEM-EDX analysis

The SEM-EDX instrument used was SEM-EDX, FEI Inspect-S50, equipped with EDX analysis from AMATEX EDAX Type Element (USA) at the Materials Laboratory, University of Malang. The SEM is complemented with an Energy Dispersive X-ray device, which uses high-speed electron shots with a 15-20 kV voltage. Morphological analysis can produce images up to 1,000,000x. The EDX analysis of AMATEX EDAX Type Element uses a Silicon Drift detector (SDD)<sup>28, 39</sup>.

### Carbon absorption capacity analysis

This study aims to test the carbon absorption capacity of iron in drilled well water using the ASC-7000, ASC Shimadzu (Japan), at the Materials Laboratory, University of Malang.

### XRD analysis

## Results and Discussion

### FTIR analysis

FTIR analysis determines the functional groups present and lost after carbon is activated based on the absorption band pattern (wavenumber;  $\nu$ ,  $\text{cm}^{-1}$ ). The results of the FTIR characterization of pyrolyzed walnut shell carbon as control and KCl-activated are shown in Fig. 1, and their interpretations are shown in Table 1. The FTIR spectrum of KCl-activated walnut shell carbon has different absorption band patterns. A comparison of the two spectra shows that after KCl activated carbon, there was a sharp increase in absorption intensity at the wave number  $3444.87 \text{ cm}^{-1}$ , which indicates the N-H functional group. The adsorption band  $3438 \text{ cm}^{-1}$  correspond to the N-H free group's amide or amino<sup>40</sup>. The strain absorption shift occurs at a wave number of  $2924.09 \text{ cm}^{-1}$ , which shows the aromatic C-H (Ar-H) functional group<sup>30</sup> absorption intensity. The absorption shift occurs at a wave number of  $2320.37 \text{ cm}^{-1}$ , with a moderate absorption intensity indicating the presence of the  $\text{C}\equiv\text{N}$  functional group. The absorption shift occurs at a wave number of  $1583.56 \text{ cm}^{-1}$ , and the sharp absorption intensity indicates stretching of the  $\text{C}=\text{O}$  carbonyl functional group. The  $1634\text{-}1635 \text{ cm}^{-1}$  band indicated  $\text{C}=\text{O}$  stretching of carboxyl or carbonyl groups<sup>41, 42</sup>. The absorption shift occurs at a wave number of  $1045.42 \text{ cm}^{-1}$ , which is the sharp absorption intensity of the C-O ester. The relatively extreme band at around  $1230 \text{ cm}^{-1}$  is assigned to the aromatic ester C-O bonds<sup>43- 45</sup>. The absorption intensity widens, indicating the bending of the Ar-H aromatic functional group<sup>31, 39</sup>.

X-ray diffraction analysis is a fundamental method for evaluating the carbon structure or determining the crystal structure<sup>29, 37, 39</sup>. The X-ray diffraction instrument was XRD, PANalytical X'Pert PRO (the Netherlands) at the Materials Laboratory, University of Malang. The instrument works at a wavelength of 1.54 Angstrom, a frequency of 12 Hz, and an energy of 250 eV.

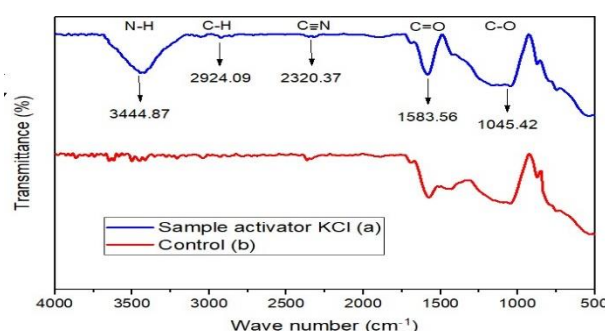


**Figure 1. FTIR spectrum of the walnut shell carbon after KCl activation (a) And before KCl activation (b).**

**Table 1. FTIR absorption band of pyrolyzed and KCl-activated walnut shell carbon.**

Wave Number ( $\text{cm}^{-1}$ )		
Results of Pyrolysis	Results of KCl-activated	Functional groups
-	3444.87	NH (stretching)
-	2924.09	Ar-H (aromatic)
-	2320.37	$\text{C}\equiv\text{N}$
1583.56	1583.56	$\text{C}=\text{O}$ (carbonyl)
1045.42	1045.42	C-O (ester)

### SEM analysis

The surface morphology structure of the carbon from the pyrolysis product of the walnut shell and after KCl activation was analyzed by Scanning Electron Microscopy (SEM), and the morphology is shown in Fig. 2 a and b. Fig. 2 shows the surface morphology of pyrolyzed and KCl-activated walnut shell carbon (c, d) with magnifications of 2000 and 5000 times, respectively. Both have different surfaces, and the pores are not uniform and irregular. This is due to the pyrolysis process and the addition of a KCl activator, resulting in an outer pore with a non-uniform surface and spreading over the entire carbon surface<sup>32</sup>. Adding a KCl solution activator to walnut shell



carbon aims to dissolve the metal elements contained in the carbon and increase the carbon content. The activation process causes many polar compounds to be released or evaporated, thereby opening carbon pores and reducing the closure of hydrocarbon pores<sup>9, 32</sup>. It appears that the pore structures are not

uniform on the carbon surface, indicating the presence of organic impurities or tar that have not evaporated<sup>18</sup>. The outer surface of the walnut shell carbon looks rough; this is related to the breakdown of the presence of heating factors at high temperatures<sup>33, 34</sup>.

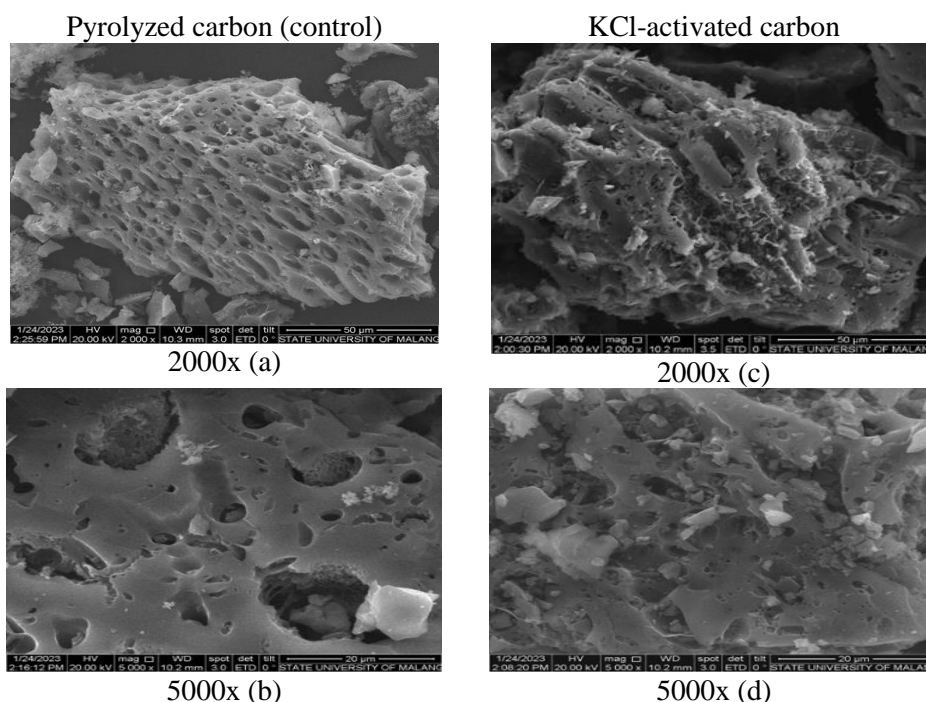


**Figure 2. SEM surface morphology of pyrolyzed (a-b) and KCl-activated walnut shell carbon (c-d) with respective magnifications of 2000x and 5000x.**

Fig. 3 shows the SEM morphology of pyrolyzed (a) and KCl-activated walnut shell carbon (b) at 10,000 magnification each. It can be seen that the pore diameters of the pyrolyzed walnut shell carbon and the activated KCl carbon vary greatly; the pore diameters are not uniform, as shown in Table 2. The pore diameter of the pyrolyzed walnut shell carbon from 145.7-757.7 nm. At the same time, the pore diameter of the KCl-activated walnut shell carbon is 1,020-1,226 µm. The other results show that using a ZnCl<sub>2</sub> activator to activate walnut shell charcoal produces a pore diameter of 22.74 µm<sup>46</sup>. The pore diameter of KCl-activated walnut shell carbon is more significant than that of the pyrolyzed one. The difference in pore diameter is quite large<sup>28</sup>. The results showed that activated walnut shell carbon pores included macropores<sup>35, 36</sup>. Other chemically bonded elements, such as oxygen and hydrogen<sup>47- 49</sup>, can also influence the pore diameter.

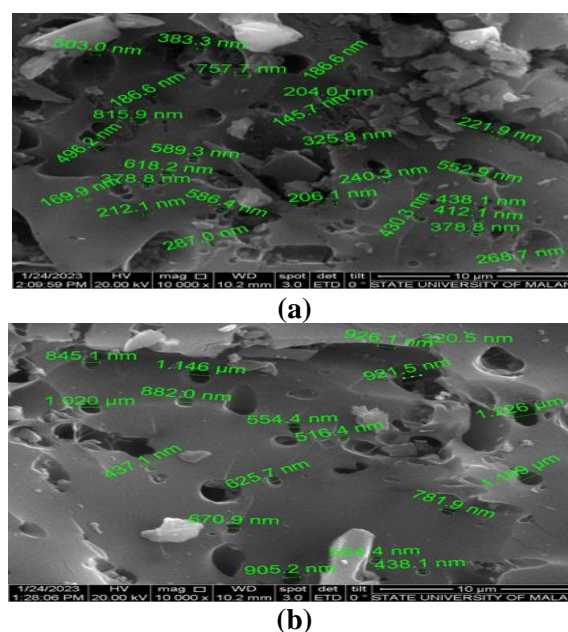


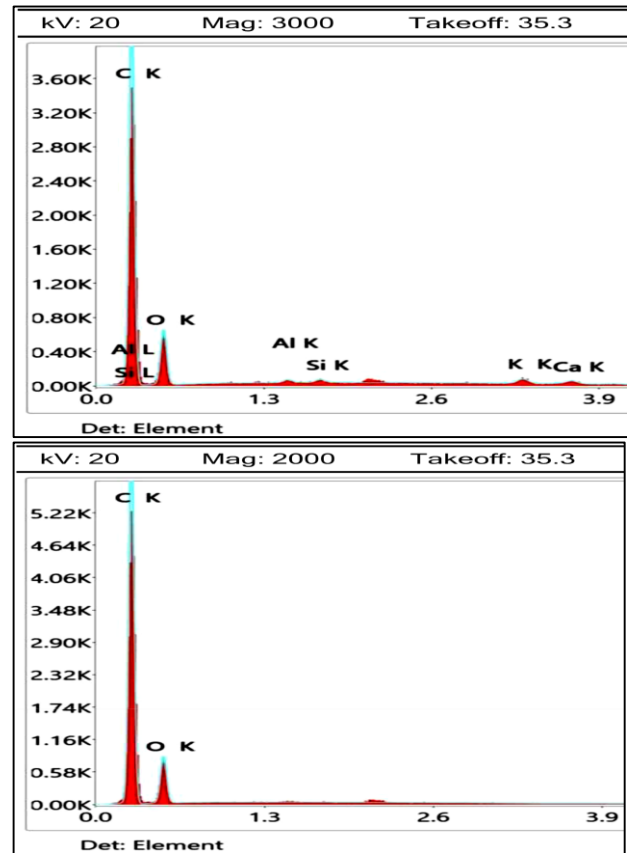
**Figure 3. SEM morphology of pyrolyzed (a) and KCl-activated walnut shell carbon (b) at 10,000x magnification.**

**Table 2. The pore diameter of pyrolyzed and KCl-activated walnut shell carbon.**

Pyrolyzed		KCl-activated	
Pore diameter	units	Pore diameter	units
212.1	nm	1,020	μm
496.2	nm	1,146	μm
145.7	nm	1,226	μm
430.3	nm	1,189	μm
206.1	nm	-	-
325.8	nm	-	-
186.6	nm	-	-
221.9	nm	-	-
757.7	nm	-	-

### EDX analysis

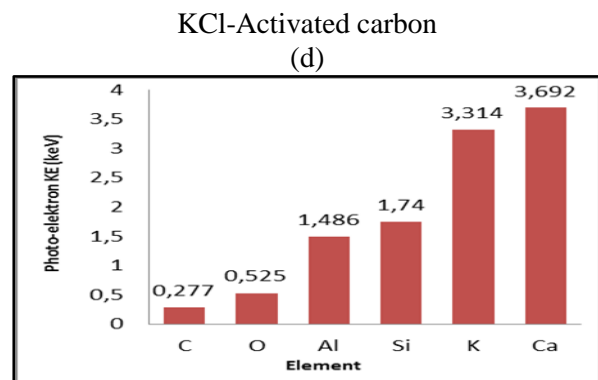
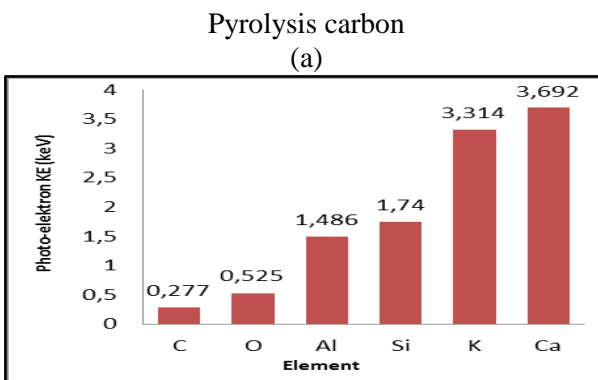
The SEM-EDX technique can identify elements of the phases seen in the microstructure images<sup>49, 50</sup>. EDX analysis of pyrolyzed and KCl-activated walnut shell carbon can be seen in Fig. 4. The graph of the photoelectron kinetic energy of the pyrolyzed walnut shell carbon and the KCl-activated walnut shell carbon in Figs. 5d-f. The magnitude of the photoelectron kinetic energy of the walnut shell carbon as a result of pyrolysis and the KCl-activated carbon are the same, as can be seen in Table 3. There is no difference in the photoelectron kinetic energy of each element, but each element has a different atomic percent and mass percent<sup>38</sup>.



**Figure 4. EDX spectrum of pyrolyzed (a) and KCl-activated walnut shell carbon (b).**

**Table 3. Results of EDX analysis of pyrolyzed and KCl-activated walnut shell carbon.**

No	Pyrolysis				KCl-activated		
	Element	Photo electron KE (keV)	Mass (%)	Atoms (%)	Photo electron KE (keV)	Mass (%)	Atoms (%)
1	C	0.277	81.10	85.40	0.277	82.80	86.50
2	O	0.525	18.10	14.30	0.525	17.20	13.50
3	Al	1.486	0.10	0.10	1.486	0.00	0.00
4	Si	1.740	0.10	0.00	1.740	0.00	0.00
5	K	3.314	0.30	0.10	3.314	0.00	0.00
6	Ca	3.692	0.30	0.10	3.692	0.00	0.00
Total		12.288	100.00	100.00	12.288	100.0	100.00



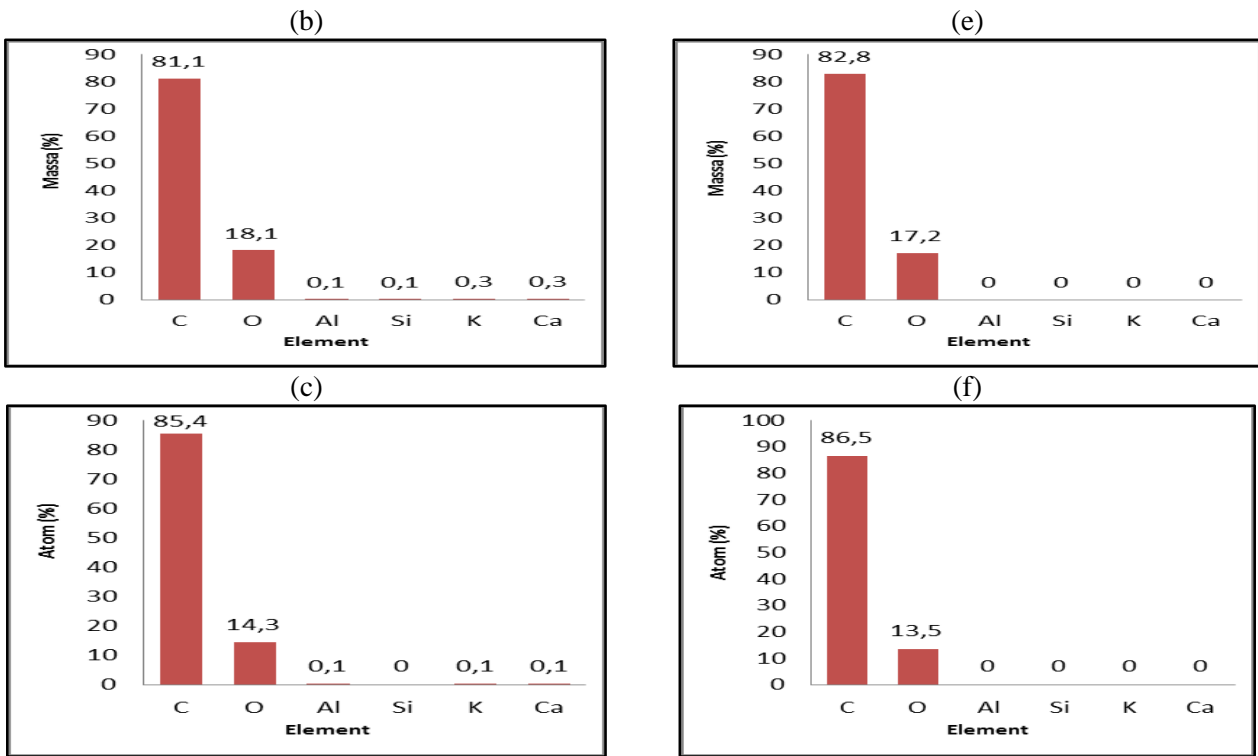


**Figure 5. Graph of (a) KE photo electrons, (b) % mass, (c) % atoms from pyrolyzed walnut shell carbon and (d) KE photo electrons, (e) % mass, (f) % atoms from KCl-activated walnut shell carbon.**

Percent (%) by mass and % of element C atoms resulting from pyrolysis of carbon were 81.10% and 85.40%, respectively. While the % mass and % atoms of carbon element C after KCl activation were 82.80% and 86.50%. O, Al, Si, K, and Ca indicate an incomplete pyrolysis or carbonization process. Compared to the other results, using a  $ZnCl_2$  salt activator to activate walnut shell charcoal produces almost the same 86.49% of C and 13.04% of O atomic mass<sup>51</sup>. The increase in pore diameter was due to the loss of impurities, namely O, Al, Si, K, and Ca. The increase in pore diameter indicated that the walnut shell carbon was getting purer after being activated with the KCl activator<sup>52,53</sup>. Consistent with the other findings, charcoal activation can enhance carbon elements' mass and atomic and molar quantities of carbon elements<sup>38</sup>.

### XRD analysis

XRD analysis was carried out to identify the crystalline phase, crystal structure, and crystallinity of the sample<sup>54</sup>. In characterization using XRD, the diffractogram of the pyrolyzed walnut shell carbon sample is observed, and the KCl-activated walnut shell carbon is shown in Fig. 6. The appearance of a broad diffraction background, irregular background intensity, and no peaks sharp edges reveal a high

amorphous structure<sup>55-57</sup>. The carbon peak of the walnut shell resulting from pyrolysis and after the carbon was activated by KCl showed a peak of  $2\theta$ , namely  $26.632^\circ$ ,  $26.702^\circ$  and  $45.502^\circ$  were significant showed crystalline and peaks of the amorphous were observed between  $2\theta = 56-90^\circ$ . They are the same as the research, namely peak  $2\theta = 49^\circ-80^\circ$ <sup>41</sup>. The scattering crystallinity of walnut shell carbon after KCl activation is higher than the scattering crystallinity of walnut shell carbon resulting from pyrolysis. They are almost the same as the other research results, namely peak  $2\theta = 23-30^\circ$ <sup>58</sup>.

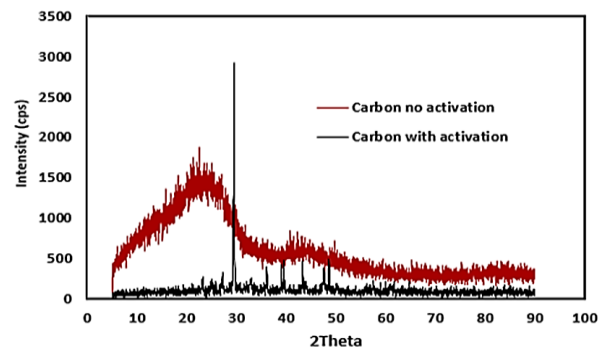


**Figure 6. Walnut shell carbon diffractogram resulting from pyrolysis (---) and diffractogram of walnut shell carbon after KCl activation (---).**

### ASC analysis

Iron (Fe) metal content measurements were carried out: a prepared test sample of drilled well water was injected into the ASC, and then the absorbance was

measured at a wavelength of 283.3 nm<sup>59- 61</sup>. The measurement results are recorded and then analyzed. The results of ASC analysis of walnut shell carbon are shown in Table 4.

**Table 4. Calculation results of Fe levels in drilled well water samples.**

No	Sample	Time (Min)	Iron metal (Fe) content (mg/L)	Metal absorbed (mg/L)	Capacity of active carbon (%)
1	Drilled well water	0	0.727	-	-
2	Drilled well water	60	0.712	0.015	2.06
3	Drilled well water	120	0.673	0.054	7.42
		150	0.605	0.122	16.78

Based on the data in Table 4, the concentration of Fe metal in drilled well water samples shows levels that are higher than the drinking water quality standards set in Minister of Health Regulation Number 492/Menkes/Per/VII/2010 with maximum iron metal content standards for drinking water of 0.3 mg/L. Compared to the other results, H<sub>3</sub>PO<sub>4</sub> charcoal produces almost the same adsorption capacity of

passiflora ligularis (PL), which was 5.07 mg/g<sup>62</sup>. The absorption capacity of activated carbon on Fe metals increased from 2.06% (60 minutes), 7.42% (120 minutes), and 16.78% (150 minutes). This means that KCl-activated walnut shell carbon can be used as an excellent absorbent for clean water treatment in the future.

### Conclusion

Based on the result from FTIR spectrums, both walnut shell carbon resulting from pyrolysis and after KCl activation show the presence of functional groups: N-H, Ar-H, aliphatic -CH<sub>3</sub> and -CH<sub>2</sub>, C≡C, carbonyl CO, ester CO, and aromatic C-H. The SEM morphology showed that the surface structure of the pyrolyzed carbon particles and carbon after KCl activation were both uneven and inhomogeneous. The results of the EDX analysis showed an increase in the amount of carbon elements after activation. The mass percentage and carbon atom percentage of the pyrolyzed walnut shell carbon were 81.10% and 85.40%, respectively, while the walnut shell carbon after KCl activation was 82.80% and 86.50%. Process chemical activation with a KCl activator can enlarge the carbon pores. Increasing the carbon composition shows that the carbon is getting purer, and the arrangement of the carbon atoms is more regular. The XRD diffractogram shows that the carbon of the pyrolyzed walnut shell and the carbon

after KCl activation both show tenuous peaks and relatively low intensities. The appearance of a diffractogram with wide diffraction, irregular diffraction intensity, and no sharp peaks reveals that the structure of the two charcoals is highly amorphous. This study highlights how waste from walnut shells can produce activated carbon, which is ideal for use as an electrode material in supercapacitors. The pyrolysis and fragmentation method of walnut shell charcoal, when used with a KCl activator, can produce activated charcoal with a macro pore size ranging from 1,020 μm to 1,226 μm. This research's novelty is that no information explicitly using KCl activator to increase the porosity of activated carbon from walnut shells is available. KCl-activated carbon can remove 0.122 mg/L of Fe(III) or 16.78% Fe(III) absorption in 150 minutes. This proves that KCl-activated walnut shell carbon can be used as an alternative absorbent for clean water treatment in the future.

### Acknowledgement

The authors thank the Department of Chemistry of Universitas Negeri Manado for providing the laboratory and some chemicals.



## Authors' Declaration

- Conflicts of Interest: None.
- We hereby confirm that all figures and tables in the manuscript are ours. Furthermore, figures and images, that are not ours, have been included with the necessary permission for re-publication, which is attached to the manuscript.
- No animal studies are present in the manuscript.
- No human studies are present in the manuscript.
- Ethical Clearance: The project was approved by the local ethical committee at Universitas Negeri Manado, Indonesia.

## Authors' Contribution Statement

I.D.K.A., C.P.M., and J.Z.L designed the study, analyzed and interpreted the data from other authors, and wrote and revised the paper. M., S.P., I.D.G.K.,

and J.J.M. performed the FTIR, SEM-EDX, XRD, and ASC analyses. C.P.M. and A.R.P.U reviewed, edited, submitted, and revised the manuscript.

## References

1. Arslan A, Zeybek Y. Using walnut shell based activated carbon for the efficient removal of phosphate from aqueous solution. *Sinop Uni J Nat Sci.* 2022 Feb; 7(1): 22-40. <https://doi.org/10.33484/sinopfdb.1013083>
2. Açıklalın K, Karaca F. Fixed-bed pyrolysis of walnut shell: Parameter effects on yields and characterization of products. *J Anal Appl Pyrolysis.* 2017 May; 125: 234-242. <http://dx.doi.org/10.1016/j.jaap.2017.03.018>
3. Sharahi M, Hivechi A, Bahrami SH, Hemmatinejad N, Milan PB. Co-electrospinning of lignocellulosic nanoparticles synthesized from walnut shells with poly (caprolactone) and gelatin for tissue engineering applications. *Cellulose.* 2021 April; 28: 4943-4957. <https://doi.org/10.1007/s10570-021-03709-w>
4. Spagnoli AA, Giannakoudakis DA, Bashkova S. Adsorption of methylene blue on cashew nut shell based carbons activated with zinc chloride: The role of surface and structural parameters. *J Mol Liq.* 2017 March; 229: 465-471. <http://dx.doi.org/10.1016/j.molliq.2016.12.106>
5. Wong S, Ngadi N, Inuwa IM, Hassan O. Recent advances in applications of activated carbon from biowaste for wastewater treatment: a short review. *J Clean Prod.* 2018 Feb; 175: 361-375. <http://dx.doi.org/10.1016/j.jclepro.2017.12.059>
6. González-García P. Activated carbon from lignocellulosics precursors: A review of the synthesis methods, characterization techniques and applications. *Renew Sustain Energy Rev.* 2018 Feb; 82(Part 1): 1393-1414. <http://dx.doi.org/10.1016/j.rser.2017.04.117>
7. Rashidi NA, Yusup S. A review on recent technological advancement in the activated carbon production from oil palm wastes. *Chem Eng J.* 2017 April; 314: 277-290. <http://dx.doi.org/10.1016/j.cej.2016.11.059>
8. Hsini A, Naciri Y, Laabd M, El Ouardi M, Ajmal Z, Lakhmiri R, et al. Synthesis and characterization of arginine-doped polyaniline/walnut shell hybrid composite with superior clean-up ability for chromium (VI) from aqueous media: Equilibrium, reusability and process optimization. *J Mol Liq.* 2020 Oct; 316: 113832. <https://doi.org/10.1016/j.molliq.2020.113832>
9. Domingos I, Ferreira J, Luísa P. Cruz-Lopes, Esteves B. Liquefaction and chemical composition of walnut shells. *Open Agric.* 2022 Feb; 7(1): 249-256. <https://doi.org/10.1515/opag-2022-0072>
10. Yusnaini, Suryanto E, Hasan S, Wulansari A, Dewi EK. The Characteristics of Volatile Compounds of Kenari (Canarium indicum L.) Shell Liquid Smoke. *IOP Conf Ser Earth Environ Sci.* 2021 March; 709(1): 012032. <http://dx.doi.org/10.1088/1755-1315/709/1/012032>
11. Olive BOS, Fabien BE, Edwige MA, Anicet NPM, Ateba A. Physico-Chemical and Thermal Characterisation of Canarium Schweinfurthii Engl (Cs) Shells. *SSRG Int J Mat Sci Eng.* 2021 Nov; 7(3): 9-15. <https://doi.org/10.14445/23948884/IJMSE-V7I3P102>
12. Maguie KA, Nsami NJ, Daouda K, Randy CN, Mbadcam KJ, Maguie K, et al. Adsorption Study of the Removal of Copper (II) Ions Using Activated Carbon Based Canarium schweinfurthii Shells Impregnated with ZnCl<sub>2</sub>. *IRA Int J Appl Sci.* 2017 Aug; 8(1): 18-30. <http://dx.doi.org/10.21013/jas.v8.n1.p2>
13. Sandi K, Syahputra RA, Zubir M. Review Journal Thermodynamics Carbon Active Adsorption Empty Fruit Bunch of Heavy Metal from Liquid Waste. *IJCST.* 2020 Sep; 3(2): 64-66. <http://dx.doi.org/10.24114/ijcst.v3i2.19530>
14. Anand S, Ahmad MW, Syed A, Bahkali AH, Verma M, Kim BH, et al. Walnut shell derived N, S co-doped activated carbon for solid-state symmetry supercapacitor device. *J Ind Eng Chem.* 2024 Jan;

- 129: 309-320.  
<https://doi.org/10.1016/j.jiec.2023.08.045>
15. Yang X, Xie D, Wang W, Li S, Tang Z, Dai S. An activated carbon from walnut shell for dynamic capture of high concentration gaseous iodine. *Chem Eng J*. 2023 Feb; 454(Part 4): 140365. <https://doi.org/10.1016/j.cej.2022.140365>
16. Serafin J, Dziejarski B, Junior OFC, Sreńscek-Nazzal J. Design of highly microporous activated carbons based on walnut shell biomass for H<sub>2</sub> and CO<sub>2</sub> storage. *Carbon*. 2023 Jan; 201: 633-647. <https://doi.org/10.1016/j.carbon.2022.09.013>
17. Khoshraftar Z, Ghaemi A. Presence of activated carbon particles from waste walnut shell as a biosorbent in monoethanolamine (MEA) solution to enhance carbon dioxide absorption. *Heliyon*. 2022 Jan; 8(1): e08689. <https://doi.org/10.1016/j.heliyon.2021.e08689>
18. Anom IDK. Kinetic Study of Gas Formation in Styrofoam Pyrolysis Process. *Acta Chimica Asiana*. 2021 Nov; 4(2): 135-140. <https://doi.org/10.29303/aca.v4i2.76>
19. Hamadeen M, Elsayed A, Elkhatib A, Mohamed E, Badawy A, Samir A, et al. Novel low cost nanoparticles for enhanced removal of chlorpyrifos from wastewater: sorption kinetics, and mechanistic studies. *Arabian J Chem*. 2021 March; 14(3): 102981. <https://doi.org/10.1016/j.arabjc.2020.102981>
20. Wang L, Guo Y, Zou B, Rong C, Ma X, Qu Y, et al. High surface area porous carbons prepared from hydrochars by phosphoric acid activation. *Bioresour Technol*. 2011 Jan; 102(2): 1947-1950. <https://doi.org/10.1016/j.biortech.2010.08.100>
21. Syafila M, Helmy Q, Musthofa AMH. Methylene blue adsorption by activated carbon and nano-activated carbon from biomass waste. *Jurnal Presipitasi : Media Komunikasi dan Pengembangan Teknik Lingkungan*. 2022 Nov; 19(3): 553-565.
22. Suliestyah, Tuheteru EJ, Yulianti R, Palit C, Yomaki CC, Ahmad SN. Production of activated carbon from coal with H<sub>3</sub>PO<sub>4</sub> activation for adsorption of Fe(II) and Mn(II) in acid mine drainage. *JDMLM*. 2024 April; 11(3): 5755-5765. <https://doi.org/10.15243/jdmlm.2024.113.5755>
23. Li X, Qiu J, Hu Y, Ren X, He L, Zhao N, et al. Characterization and comparison of walnut shells-based activated carbons and their adsorptive properties. *Adsorp Sci Technol*. 2020 Dec; 38(9-10): 450-463. <http://dx.doi.org/10.1177/0263617420946524>
24. Zhang X, Gao B, Fang J, Zou W, Dong L, Cao C, et al. Chemically activated hydrochar as an effective adsorbent for volatile organic compounds (VOCs). *Chemosphere*. 2019 March; 218: 680-686. <https://doi.org/10.1016/j.chemosphere.2018.11.144>
25. Rini DS, Prasetyo DM, Adawi TF, Aji IML, Syaputra M, Webliana K, et al. Effect of activation temperature and H<sub>3</sub>PO<sub>4</sub> concentration on activated carbon from asian palmyra palm fronds (*Borassus flabellifer* Linn). *Jurnal Multidisiplin Madani (MUDIMA)*. 2024 June; 4(6): 720-728.
26. Qiu X, Wang L, Zhu H, Guan Y, Zhang Q. Lightweight and efficient microwave absorbing materials based on walnut shell-derived nano-porous carbon. *Nanoscale*. 2017 May; 9(22): 7408-7418. <https://doi.org/10.1039/C7NR02628E>
27. Yu Q, Li M, Ning P, Yi H, Tang X. Preparation and phosphine adsorption of activated carbon prepared from walnut shells by KOH chemical activation. *Sep Sci Technol*. 2014 Sep; 49(15): 2366-2375. <http://dx.doi.org/10.1080/01496395.2014.917326>
28. Raymundo-Pinero E, Azaïs P, Cacciaguerra T, Cazorla-Amorós D, Linares-Solano A, Béguin F. KOH and NaOH activation mechanisms of multiwalled carbon nanotubes with different structural organization. *Carbon*. 2005 Dec; 43(4): 786-795. <http://dx.doi.org/10.1016/j.carbon.2004.11.005>
29. Bhat VS, Krishnan SG, Jayeoye TJ, Rujiralai T, Sirimahachai U, Viswanatha R, et al. Self-activated green carbon nanoparticles for symmetric solid-state supercapacitors. *J Mater Sci*. 2021 May; 56: 13271-13290. <https://doi.org/10.1007/s10853-021-06154-z>
30. Farma R. Physical properties analysis of activated carbon from oil palm empty fruit bunch fiber on methylene blue adsorption. *Journal of Technomaterial Physics (JoTP)*. 2019 Feb; 1(1): 67-73. <https://doi.org/10.32734/jotpv1i1.824>
31. Prayogatama A, Nuryoto N, Kurniawan, T. Modifikasi Karbon Aktif dengan Aktivasi Kimia dan Fisika Menjadi Elektroda Superkapasitor. *J Sains Teknologi*. 2022 Feb; 11(1): 47-58. <https://doi.org/10.23887/jstundiksha.v11i1.42849>
32. Lu SG, Bai SQ, Zhu L, Shan HD. Removal mechanism of phosphate from aqueous solution by fly ash. *J Hazard Mater*. 2009 April; 161(1): 95-101. <http://dx.doi.org/10.1016/j.jhazmat.2008.02.123>
33. Saputra A, Rina O, Hidayat R, Fitria M, Akhni SA, Purnomo A, et al. Synthesis of bamboo-based activated carbon through physicochemical activation for coal-runoff wastewater treatment. *IJCA*. 2023 Sep; 6(2): 143-150. <https://doi.org/10.20885/ijca.vol6.iss2.art6>
34. Azmi NZM, Buthiyappan A, Raman AAA, Patah MFA, Sufian S. Recent advances in biomass based activated carbon for carbon dioxide capture—A review. *J Ind Eng Chem*. 2022 Dec; 116: 1-20. <https://doi.org/10.1016/j.jiec.2022.08.021>
35. Merin P, Jimmy Joy P, Muralidharan MN, Veena Gopalan E, Seema A. Biomass-derived activated carbon for high-performance supercapacitor electrode applications. *Chem Eng Technol*. 2021 Jan; 44(5): 844-851. <http://dx.doi.org/10.1002/ceat.202000450>
36. Zhang S, Song B, Cao C, Zhang H, Liu Q, Li K, et al. Structural evolution of high-rank coals during

- coalification and graphitization: X-ray diffraction, Raman spectroscopy, high-resolution transmission electron microscopy, and reactive force field molecular dynamics simulation study. *Energ Fuel*. 2021 Jan; 35(3): 2087-2097. <https://doi.org/10.1021/acs.energyfuels.0c03649>
37. Kunusa WR, Iyabu H, Abdullah R. FTIR, SEM and XRD analysis of activated carbon from sago wastes using acid modification. *J Phys: Conf Ser*. 2021 July; 1968(1): 012014. <http://dx.doi.org/10.1088/1742-6596/1968/1/012014>
38. Rampe MJ, Santoso IRS, Rampe HL, Tiwow VA, Rorano TEA. Study of pore length and chemical composition of charcoal that results from the pyrolysis of coconut shell in Bolaang Mongondow, Sulawesi, Indonesia. *Karbala Int J Mod Sci*. 2022 Feb; 8(1): 96-104. <https://doi.org/10.33640/2405-609X.3208>
39. Joni R, Syukri, Hermansyah A. Study of activated carbon characteristic from ketaping fruit shell (*Terminalia Catappa*) as supercapacitors electrode. *JAcPS*. 2021 Jan; 10(1): 1-6. <https://doi.org/10.24815/jacps.v10i1.17755>
40. Bougheriou F, Ghoualem H. Synthesis and characterization of activated carbons from walnut shells to remove diclofenac. *Iran J Chem Eng*. 2023 Sep; 42(9): 2812-2832. <https://doi.org/10.30492/ijcce.2023.559588.5499>
41. Dungani R, Munawar SS, Karliati T, Malik J, Aditiawati P, Sulistyono. Study of characterization of activated carbon from coconut shells on various particle scales as filler agent in composite materials. *J Korean Wood Sci Technol*. 2022 June; 50(4): 256-271. <https://doi.org/10.5658/WOOD.2022.50.4.256>
42. Mahdi SM, Faisal ML, Al-Sharify ZT, Onyeaka H. Walnut shells as sustainable adsorbent for the removal of medical waste from wastewater. *J Eng Sustain Dev*. 2023 Nov; 27(6): 698-712. <https://doi.org/10.31272/jeasd.27.6.3>
43. Wu Z, Sun Z, Liu P, Li Q, Yanga R, Yanga X. Competitive adsorption of naphthalene and phenanthrene on walnut shell based activated carbon and the verification via theoretical calculation. *R Soc Chem Adv*. 2020 March; 10: 10703-10714. <https://doi.org/10.1039/C9RA09447D>
44. Oba OA, Aydinlik NP. Preparation of mesoporous activated carbon from novel african walnut shells (AWS) for deltamethrin removal: Kinetics and equilibrium studies. *Appl Water Sci*. 2022 May; 12(149): 1-20. <https://doi.org/10.1007/s13201-022-01672-w>
45. Kim JJ, Ling FT, Plattenberger DA., Clarens AF, Lanzirrotti A, Newville M, et al. SMART mineral mapping: Synchrotron-based machine learning approach for 2D characterization with coupled micro XRF-XRD. *Comput Geosci*. 2021 Nov; 156: 104898. <https://doi.org/10.1016/j.cageo.2021.104898>
46. Jery AE, Khedher KM, Salman HM, Al-Ansari N, Sammen SS, Scholz M. Thermodynamic and structural investigation of oily wastewater treatment using peach kernel and walnut shell based activated carbon. *Plos One*. 2024 May; 19(5): e0297024. <https://doi.org/10.1371/journal.pone.0297024>
47. Yan L, Liu Y, Hou J. High-efficiency oxygen reduction reaction revived from walnut shell. *Molecules*. 2023 Feb; 28(5): 2072. <https://doi.org/10.3390/molecules28052072>
48. Gan YX. Activated carbon from biomass sustainable sources. *Carbon*. 2021 April; 7(39): 1-33. <https://doi.org/10.3390/c7020039>
49. Duan XH, Srinivasakannan C, Yang KB, Peng JH, Zhang LB. Effects of heating method and activating agent on the porous structure of activated carbons from coconut shells. *Waste Biomass Valori*. 2012 June; 3: 131-139. <http://dx.doi.org/10.1007/s12649-011-9097-z>
50. Yağmur HK, Kaya İ. Synthesis and characterization of magnetic ZnCl<sub>2</sub>-activated carbon produced from coconut shell for the adsorption of methylene blue. *J Mol Struct*. 2021 May; 1232: 130071. <https://doi.org/10.1016/j.molstruc.2021.130071>
51. Yadav R, Macherla N, Singh K, Kumari K. Synthesis and electrochemical characterization of activated porous carbon derived from walnut shells as an electrode material for symmetric supercapacitor application. *Eng Proc*. 2024 Jan; 59(1): 175. <https://doi.org/10.3390/engproc2023059175>
52. Georjin J, Pinto D, Franco DS, Schadeck Netto M, Lazarotto JS, Allasia DG, et al. Improved adsorption of the toxic herbicide diuron using activated carbon obtained from residual cassava biomass (*Manihot esculenta*). *Molecules*. 2022 Nov; 27(21): 7574. <https://doi.org/10.3390/molecules27217574>
53. Inbaraj BS, Sridhar K, Chen BH. Removal of polycyclic aromatic hydrocarbons from water by magnetic activated carbon nanocomposite from green tea waste. *J Hazard Mater*. 2021 Aug; 415: 125701. <https://doi.org/10.1016/j.jhazmat.2021.125701>
54. Zhan Y, Zhou H, Guo F, Tian B, Du S, Dong Y, et al. Preparation of highly porous activated carbons from peanut shell as low-cost electrode materials for supercapacitors. *J Energy Storage*. 2021 Feb; 34: 102180. <https://doi.org/10.1016/j.est.2020.102180>
55. Uzosike AO, Ofudje EA, Akiode OK, Ikenna CV, Adeogun AI, Akinyele JO, et al. Magnetic supported activated carbon obtained from walnut shells for bisphenol-a uptake from aqueous solution. *Appl Water Sci*. 2022 July; 12(201): 1-16. <https://doi.org/10.1007/s13201-022-01724-1>
56. Riyanto CA, Ampri MS, Martono Y. Synthesis and Characterization of Nano Activated Carbon from Annatto Peels (*Bixa orellana* L.) Viewed from Temperature Activation and Impregnation Ratio of H<sub>3</sub>PO<sub>4</sub>. *Eksata: Journal of Sciences and Data Analysis*

- 2020 Feb; 1(1): 44-50.  
<https://doi.org/10.20885/EKSAKTA.vol1.iss1.art7>
57. Shrestha LK, Adhikari L, Shrestha RG, Adhikari MP, Adhikari R, Hill JP, et al. Nanoporous carbon materials with enhanced supercapacitance performance and non-aromatic chemical sensing with C1/C2 alcohol discrimination. *Sci Technol Adv Mat.* 2016 Sep; 17(1): 483-492.  
<https://doi.org/10.1080/14686996.2016.1219971>
58. Iwanow M, Gärtner T, Sieber V, König B. Activated carbon as catalyst support: precursors, preparation, modification and characterization. *Beilstein J Org Chem.* 2020 June; 16: 1188-1202.
59. Suryadirja A, Muliarsi H, Ananto AD, Andayani Y. Analysis of Iron (Fe) Levels in Drilling Well Water in Praya Tengah District Using Atomic Absorption Spectrophotometry. *J Kireka.* 2021 Dec; 2(1): 146-153.  
<https://doi.org/10.31001/jkireka.v2i1.21>
60. Hupian M, Galamboš M, Viglašová E, Roskopfová O, Kusumkar VV. Activated carbon treated with different chemical agents for pertechnetate adsorption. *J Radioanal Nucl Chem.* 2024 Feb; 333: 1815-1829.  
<https://doi.org/10.1007/s10967-024-09399-5>
61. Kristianingrum S, Sulistyani, Larastuti AR. The effectiveness of active carbon adsorbent of cassava peel (*Manihot esculenta* crantz) in reduce level of chromium metal in tannery liquid waste. *Indo J Chem Env.* 2022 Dec; 5(2): 58-67.  
<http://dx.doi.org/10.21831/ijoc.v5i2.18813>
62. Santos JSD, Umpire PP, Dueñas RA, Merma WV, Andia JM. Preliminary studies of arsenic adsorption using activated carbons synthesized from *Kagneckia lanceolata* and *Passiflora ligularis*. *Int J Environ Sci Dev.* 2024 Feb; 15(1): 44-50.  
<https://doi.org/10.18178/ijesd.2024.15.1.1466>

## تشخيص الكربون المنشط بكلوريد البوتاسيوم المشتق من قشور الجوز في جزيرة تيدور، إندونيسيا

ديوي كيتوت أنوم<sup>1</sup>، تشاليب بول ماناري<sup>1</sup>، ماريانوس<sup>2</sup>، جوني زيت لومبوك<sup>1</sup>، سابريزال هاديسابوترا<sup>3</sup>، ديوا جيدي كاتجا<sup>4</sup>، جيفري جاك مامانكي<sup>5</sup>، أيسيا ريسوتوتينيسيه بوتري أوتامي<sup>1</sup>

- 1 قسم الكيمياء، كلية الرياضيات والعلوم الطبيعية، جامعة نيجري مانادو، إندونيسيا.  
2 قسم الفيزياء، كلية الرياضيات والعلوم الطبيعية، جامعة نيجري مانادو، إندونيسيا.  
3 قسم تعليم الكيمياء، كلية تدريب المعلمين والتعليم، جامعة ماتارام، إندونيسيا.  
4 قسم الكيمياء، كلية الرياضيات والعلوم الطبيعية، جامعة سام راتولانجي، إندونيسيا.  
5 قسم الأحياء، كلية الرياضيات والعلوم الطبيعية، جامعة نيجيري مانادو، إندونيسيا.

### الخلاصة

يعتبر الكربون المنشط ذو قيمة عالية لتعدد استخداماته واستخدامه الصناعي الواسع النطاق. ينتج الجوز (*Canarium vulgare* Leech)، وهو نبات إندونيسي أصلي يوجد بشكل أساسي في المناطق الشرقية مثل جزر مالوكو وتيدور، قشورًا يمكن تحويلها إلى كربون نشط. تضمنت هذه الدراسة الحصول على الكربون من قشور الجوز من خلال التحلل الحراري عند 360 درجة مئوية لمدة 6 ساعات، يليه التنشيط في محلول 3 M KCl لمدة 24 ساعة. تم تحليل الكربون المنشط باستخدام مطيافية تحويل فورييه بالأشعة تحت الحمراء (FTIR)، ومجهر مسح إلكتروني - أشعة سينية مشننة للطاقة (SEM-EDX)، وحيود الأشعة السينية (XRD). كشف تحليل FTIR عن مجموعات وظيفية بما في ذلك N-H و Ar-H (عطري) و C≡N وكربونيل CO وإستر CO. أظهرت صور المجهر الإلكتروني الماسح بنية غير متجانسة في الكربون المنشط بالتحلل الحراري و KCl بعد التنشيط، زاد توزيع قطر المسام بشكل ملحوظ من 496.2 نانومتر إلى 1226 ميكرومتر. أشار تحليل EDX إلى ارتفاع في محتوى الكربون من 85.40% بعد التحلل الحراري إلى 86.50% بعد تنشيط كلوريد البوتاسيوم. اقترحت حيود الأشعة السينية هيكل غير متبلورة في كلا الشكلين من الكربون، كما هو موضح من خلال القمم السائبة وأنماط الحيود العريضة. يقدم هذا البحث الاستخدام الجديد لكلوريد البوتاسيوم كمنشط لتعزيز مسامية الكربون المنشط المشتق من قشور الجوز. أظهر الكربون المنشط بكلوريد البوتاسيوم القدرة على إزالة 0.122 مجم / لتر من Fe (III)، محققًا امتصاص 16.78% من Fe (III) في 150 دقيقة. تشير هذه النتائج إلى أن كربون قشور الجوز المنشط بكلوريد البوتاسيوم يمكن أن يكون بديلاً فعالاً للامتصاص لمعالجة المياه النظيفة في المستقبل.

الكلمات المفتاحية: الكربون، FTIR، منشط كلوريد البوتاسيوم، EDX-SEM، قشور الجوز، XRD.